Spectral, mechanical, dielectric and third order NLO properties of diglycine magnesium sulfate crystals

P.Manimekalai[1*] and P.Selvarajan[2]

[1]Department of Physics, Christ The King Polytechnic College, Othakkalmandapam, Coimbatore-641032, India

.

[2]Department of Physics, Aditanar College of Arts and Science, Tiruchendur-628216, India.

*Corresponding author: P.Manimekalai[1]

Abstract

A third-order nonlinear optical (NLO) crystal viz. diglycine magnesium sulfate (DGMS) crystal has been grown by solution method using aqua solution. Solubility and metastable zone width for the sample were measured. The grown crystal was subjected to single crystal XRD studies to identify the crystal structure. From SHG studies, it is confirmed that the grown DGMS crystal is centrosymmetric material and hence it does not give SHG. Mechanical parameters such as hardness, yield strength, stiffness constant of the sample were measured. Values of dielectric constant, loss factor and AC conductivity were determined as a function of frequency and temperature and hence activation energy for DGMS crystal was evaluated. Third-order NLO parameters were for the grown crystal of DGMS were obtained by Z-scan technique. UV-visible spectral studies were carried out for the sample and optical parameters such as absorbance, reflectance and optical band gap were evaluated. The elements present in the sample were confirmed by EDAX and CHN analyses. Laser damage threshold (LDT) value was measured for DGMS crystal using a Nd:YAG laser.

Key words: Crystal growth; NLO; XRD; Hardness; Z-scan; Dielectrics; LDT

1. Introduction

Nonlinear optical (NLO) materials have been playing an important role in generating second harmonic, third harmonic and higher harmonic laser light and they are useful in optical computing, optical communication, optical data storage and processing. Mainly, NLO crystals are classified into centrosymmetric and non-centrosymmetric crystals. Centrosymmetric NLO crystals can generate third-order or other odd-order harmonic generations and non-centrosymmetric NLO crystals can generate second-order, third-order and other all-order harmonic generations of laser light if they are irradiated with an infrared laser light [1-3]. Many researchers are actively involved in using amino acids like glycine, L-

alanine, L-arginine, L-histidine, L-threonine, L-proline etc to prepare novel second-order and third-order NLO crystals for usage in laser, optical and photonic technologies[4-10].

Among amino acids, glycine has the non-chiral zwitterionic form and it crystallizes in six different polymeric forms viz. α, β, γ, δ, ε and β' - forms. α-glycine has no asymmetric carbon atom and is optically inactive. It has been reported that glycine combines with sulpuric acid, nitric acid, calcium chloride, calcium nitrate, barium chloride, silver nitrate, phosphoric acid, lithium sulfate, sodium nitrate, hydrochloric acid etc to form useful single crystals [11-17]. In this work, glycine is combined with magnesium sulfate to produce diglycine magnesium sulfate crystal and it is subjected to various studies. From XRD studies, it is confirmed that the grown diglycine magnesium sulfate crystal is a centrosymmetric crystal and it has the third-order nonlinear optical properties and the third-order nonlinear susceptibilities are indispensable for all optical switching, modulating, and computing devices [18]. The third-order nonlinear optical materials have weak nonlinear absorption but strong nonlinear refraction and have considerable attention of their potential use in the optical signal processing devices [19]. The aim of this work is to report third-order NLO studies and other studies of diglycine magnesium sulfate crystals grown by solution method with slow evaporation technique.

2. Experimental methods

Glycine and magnesium sulfate were taken in the stoichiometric ratio 2:1 and the required quantity of the reactants were dissolved in the double distilled water to prepare the saturated solution. The solution was stirred for about to 2 hours using a hot plate magnetic stirrer to ensure homogeneous temperature and concentration over entire volume of the solution. The solution was filtered and transferred to a crystal growth vessel and crystallization was allowed to take place by slow evaporation. Transparent, colorless crystals were harvested in a period of 25 days.

3. Results and discussion

3.1 Measurement of solubility and metastable zone width

Solubility is defined as the amount of solute in grams present in 100 ml of saturated solution at a particular temperature and it corresponds to saturation between a solid and its solution at the given temperature and pressure. The grown crystal of diglycine magnesium sulfate (DGMS) was finely powdered and used for the solubility study. A known amount of the solvent was taken in a beaker and the saturated solution was prepared using the double distilled water as the solvent by adding the sample. After attaining the saturation, 10 ml of the solution was taken in a petri dish and the solvent was evaporated by heating it slightly and then the solubility was determined gravimetrically [20]. The solubility of the sample in water was determined at different temperatures in the range 30 - 60 °C. The measurement of metastable width (MSZW) was carried out by the polythermal method [21] by using a constant cooling rate to generate supersaturation and the nuclei are detected visually. The studies were carried out in a constant temperature bath controlled to an accuracy of +0.01 °C provided with a cryostat for cooling below room temperature. A constant volume of 10 ml of solution was used to find MSZW. The solution was preheated to 5 ^{o}C above the saturated temperature for homogenization. The equilibrium saturated solution is cooled from the overheated temperature and the temperature at which the first visible crystal nucleus in the solution is noted and this is the nucleation temperature. This experiment was carried out for the solution saturated at 30, 40, 50 and 60 ^{o}C. Repeated trials were performed to ascertain the correctness of the observed results. The solubility curve and the nucleation curve for DGMS sample are given in the Fig. 1. It is observed from the results that the solubility increases with temperature and hence the sample has a positive temperature coefficient of

solubility. Solubility of a material in a particular solvent defines the supersaturation which is the driving force for the rate of crystal growth. The MSZW is the difference between the saturation and the nucleation temperatures. For less solubility, growth rate will be small and hence size of crystal will be also small. Metastable zone width (MSZW) is a basic and an important parameter in terms of temperature for growing a crystal by solution growth technique. The MSZW is strongly influenced by a number of factors such as temperature, thermal history, cooling rate, experimental setup, measuring technique, nature of solution, pH, mechanical effect and presence of impurities.

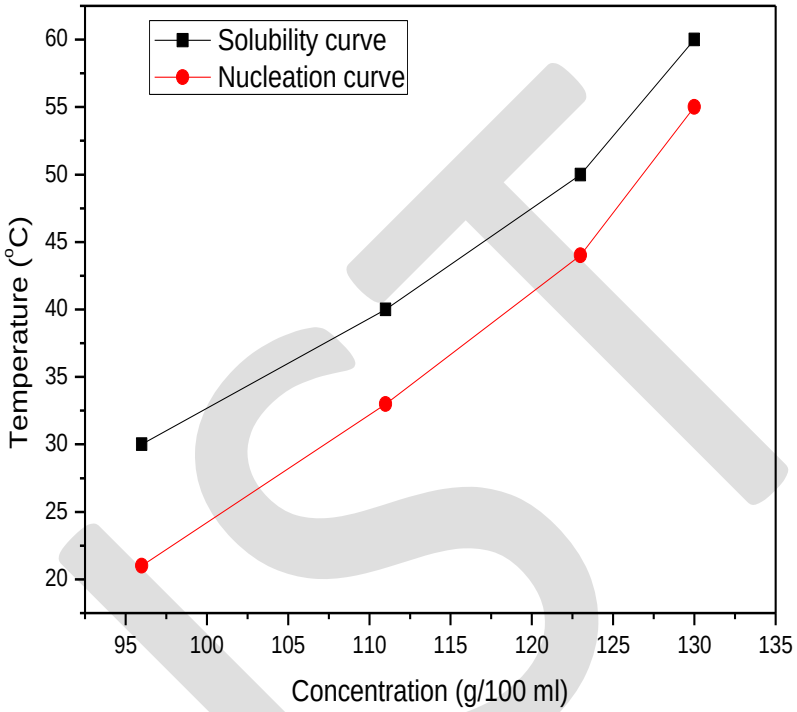

Fig.1: Solubility and nucleation curves for diglycine magnesium sulfate crystal

3.2 SHG studies

The second harmonic generation (SHG) behavior of the powdered material was tested using the Kurtz and Perry method [22]. A high intensity Nd:YAG laser (λ = 1064 nm) with a pulse duration of 6 ns was passed through the powdered sample of diglycine magnesium sulfate. From the experiment, it is noticed that there is no green light (no SHG emission) emitted from the sample and it concluded that diglycine magnesium sulfate is not a second harmonic generator.

3.3 Single crystal XRD studies

Single crystal X-ray diffraction (SCXRD) technique is used find the detailed information about the internal lattice of crystalline substances, including unit cell dimensions, bond lengths, bond angles, and details of site-ordering. Single crystal XRD analysis of grown diglycine magnesium sulfate (DGMS) has been carried out

using ENRAF NONIUS CAD-4 X-ray diffractometer and the obtained crystallographic data are given in the table 1. From results, it is observed that DGMS crystal belongs to centrosymmetric triclinic crystal system. Number of molecules per
unit cell (Z) and the density of the DGMS crystal (ρ) are 2 and 1.241 g/cc respectively. Since DGMS crystal is a centrosymmetric crystal, it does not give SHG
and it is confirmed from SHG studies.

Table 1: Single crystal XRD data of diglycine magnesium sulfate crystal

Identification code	DGMS
Molecular weight	195.4
Crystal color	Colorless, transparent
Symmetry	Triclinic
Space group	P-1
A	6.002(2) Å
B	6.697(3 Å
C	13.295 (4) Å
α	86.34 (2)^{o}
β	83.45(4)°
γ	88.74 (3)
Z	2
Volume	523.25(3) Å^{3}
Density	1.241 g/cc
Diffractometer	BRUKER-NONIUS CAD4
Radiation wavelength	K-Alpha 0.71073Å
Refinement method	Full matrix least square method

3.4 Microhardness, yield strength and stiffness constant

The mechanical strength of crystals was tested by carrying out microhardness studies by applying different low loads. The hardness of a solid is defined as its resistance to local plastic/permanent deformation and the simplest way to obtain it is to press a hard indenter of

known geometry and to divide the applied load (P) by the area (A) of the indentation produced, i.e. hardness = P/A. The hardness of a material is usually calculated from the measured value of indentation diagonal length (d) produced by an applied load. The mean diagonal length of the indentation or impression was measured using a LEITZ microhardness tester, fitted with a Vickers diamond pyramidal indenter. The well polished crystal was placed on the platform of Vickers microhardness tester and the loads of different magnitudes were applied in a fixed interval of time. The indentation time was kept 10 s for all the loads. For each load, several indentations were made and the average value of the diagonal length (d) was used to calculate the microhardness.Vickers microhardness number was determined using the relation $H_v = 1.8544\ P/d^2$ where P is applied load and d is diagonal length of indentation impression. The plot H_v versus P is shown in the figure 2. It is observed from the results that the hardness number was found to increase with the load. This can be explained qualitatively on the basis of depth of penetration of the indenter. For small loads, only a few surface layers are penetrated by the indenter. The measured hardness is the characteristics of this layer and H_v increases with load in this region. With increase in load, the overall effect is due to surface as well as inner layers of the sample. Yield strength of the material can be found out using the relation, yield strength $(\sigma_y) = (H_v / 3)$ and the stiffness constant (C_{11}) for different loads was calculated the formula $C_{11} = H_v^{7/4}$ where H_v is the microhardness number of the sample. The plots of yield strength and stiffness constant versus the applied are presented in the figure 3. Since this crystal has reverse indentation size effect the hardness, yield strength and stiffness constant values increase with increase of applied load [23,24].

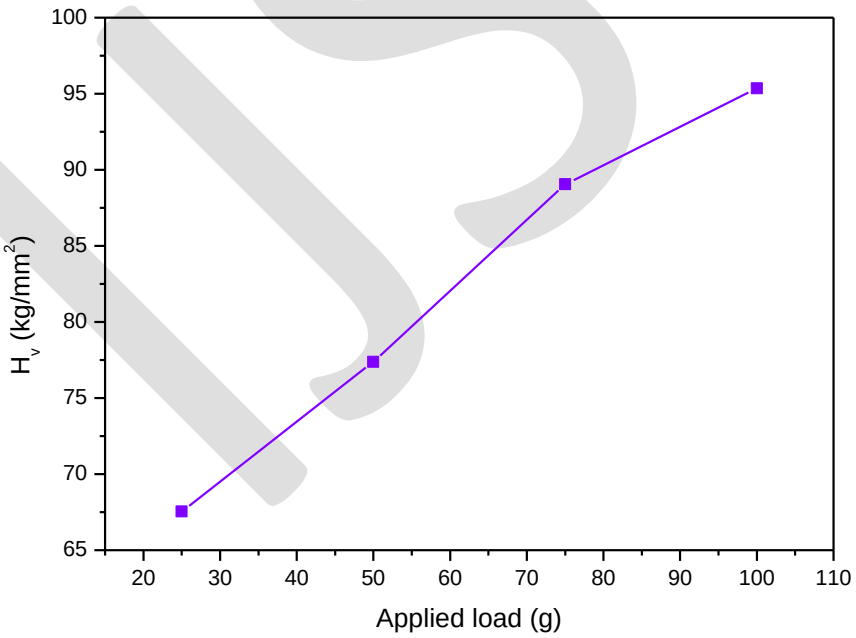

Fig.2: Variation of microhardness number with the applied load for diglycine magnesium sulfate crystal

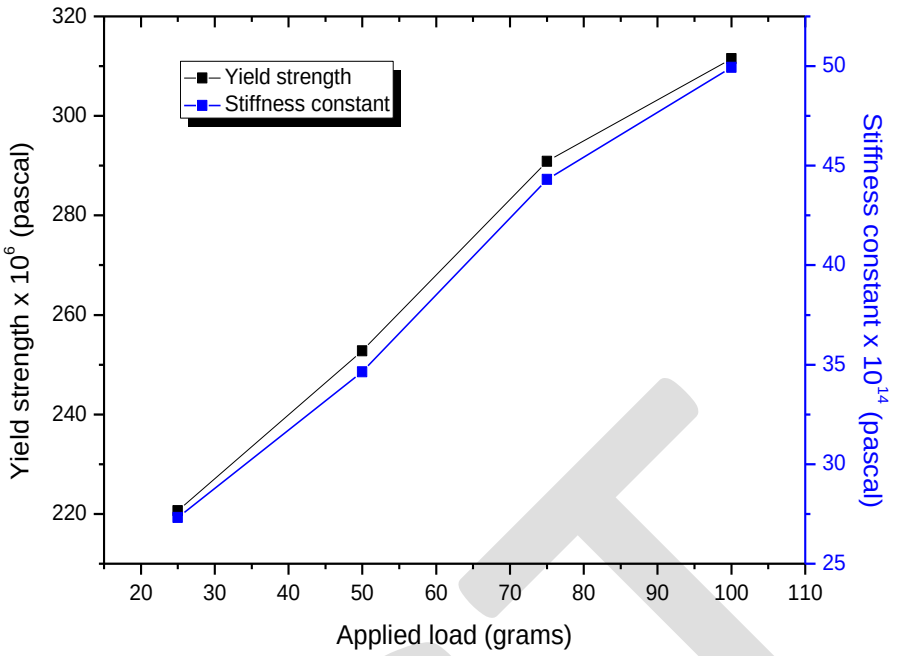

Fig.3: Variations of yield strength and stiffness constant with the applied load for diglycine magnesium sulfate crystal

3.5 Dielectric studies

Dielectric study concerns storage and dissipation of electric energy under the influence of electric field. The electric response of a dielectric can be explained by its dielectric strength, polarization, conductivity, dielectric loss, and dielectric constant. The values of dielectric constant and dielectric loss were measured using an LCR meter (Model: Agilent 4284A) at different frequencies and temperatures. The variations of dielectric constant (ε_r) and dielectric loss (tan δ) with frequency at room temperature (30 ^oC) are shown in the figures 4 and 5. The high values of ε_r at low frequencies may be due to presence of space charge polarization and its low value may be due to the reduction of polarizations at higher frequencies. It is to be noted here that space charge polarization is dominant whereas electronic and ionic polarizations are not very much active in low frequency range. The decrease in dielectric permitivity with frequency can be attributed to the contribution of the multicomponent polarizability, which are deformational and relaxation. Deformational polarizability is the mutual displacement of the oppositely charged particles under the action of applied field. On the other hand, the relaxation polarizability originated from limited mobility of the permanent dipoles lower frequencies. In other words, as the frequency increases dipoles will no longer be able to rotate sufficiently, so that their oscillation will begin to lag behind those of the field. Temperature dependent of dielectric constant and loss factor of the sample at frequencies 10^3 and 10^5 Hz are presented in the figures 6 and 7. The increase of dielectric constant as the temperature increases in the samples is due to the increase of the space charge polarizaton due to thermally generated carriers. From the results, it is observed that the behavior of dielectric loss factor is the same as that of dielectric constant. Low value of dielectric loss at low temperatures indicates that the grown crystal of DGMS is of good quality dielectric material [25].

AC conductivity is an important parameter for the dielectric material and it is determined using for relation $\sigma_{ac} = 2\pi f \varepsilon_o \varepsilon_r \tan\delta$ where ε_o is the permittivity of free space, ε_r is the dielectric constant of the sample, $\tan\delta$ is the dielectric loss of the sample and f is the frequency of AC signal. The calculated values of AC conductivity for the sample for different temperatures at frequencies 10^3 and 10^5 Hz are shown in the figure 8. The results show that AC conductivity increases with increase of temperature and frequency. When the temperature is increased the ionic distance in the sample will be increased and hence there is an increase of polarization so the conductivity increases for increase of temperature. The energy needed to form the defect is much larger than the energy needed for its drift. For many substances, as the temperature increases more and more defects are produced which in turn, increases the conductivity. The intrinsic defects caused by thermal fluctuations in a crystal determine the conductivity of a crystal. When the temperature of the crystal is increased, there is a possibility of weakening of bonds in the sample and hence this results in an enhanced conductivity in the material as the temperature increases [26].

The temperature dependence of AC conductivity is usually obeying the well known relation $\sigma_{ac} = \sigma \exp(-E_{ac}/kT)$ where k is the Boltzmann's constant, T is the absolute temperature, σ is the constant depending on the material and E_{ac} is the AC activation energy. The above equation can be written as $\ln \sigma_{ac} = \ln \sigma - E_{ac}/kT$. This is the equation for a straight line. A plot of $\ln \sigma_{ac}$ versus (1/T) gives E_{ac}/kT as the slope and $\ln \sigma$ as the Y-intercept. It is customary to plot $\ln \sigma_{ac}$ versus (1000/T), from the slope of which the activation energy (E_{ac}) can be calculated [27]. The plots of σ_{ac} versus 1/T for DGMS crystal are shown in the figure 9. The obtained values of the activation energy (E_{ac}) are 0.286 eV and 0.274 eV for the frequencies 10^3 and 10^5 Hz respectively. Since the values of conductivity of the sample at 10^5 Hz are more than 10^3 Hz, the value of activation energy is less for 10^5 than that for 10^3 Hz

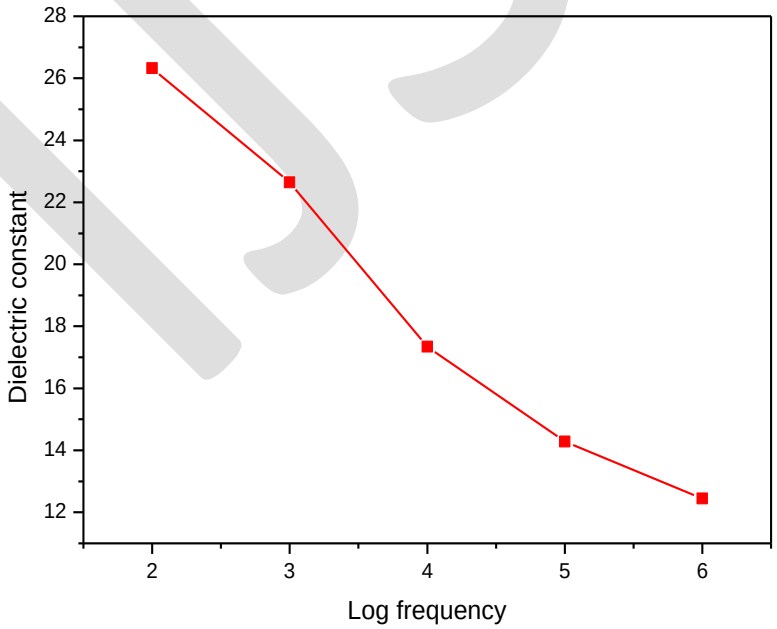

Fig.4: Variation of dielectric constant with frequency for diglycine magnesium sulfate crystal at 30 ^oC

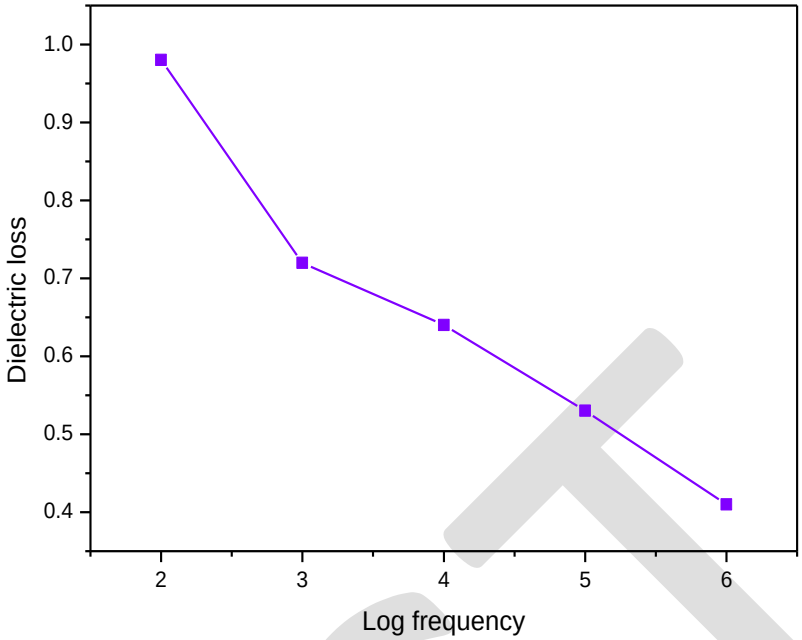

Fig.5: Variation of dielectric loss with frequency for diglycine magnesium sulfate crystal at 30 ^{o}C

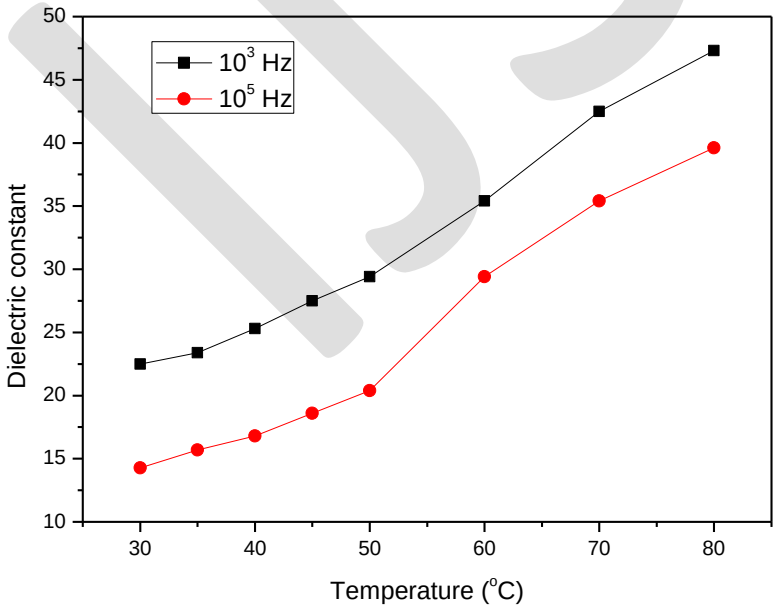

Fig.6: Variation of dielectric constant with temperature at frequencies of $10^3$and 10^5 Hz

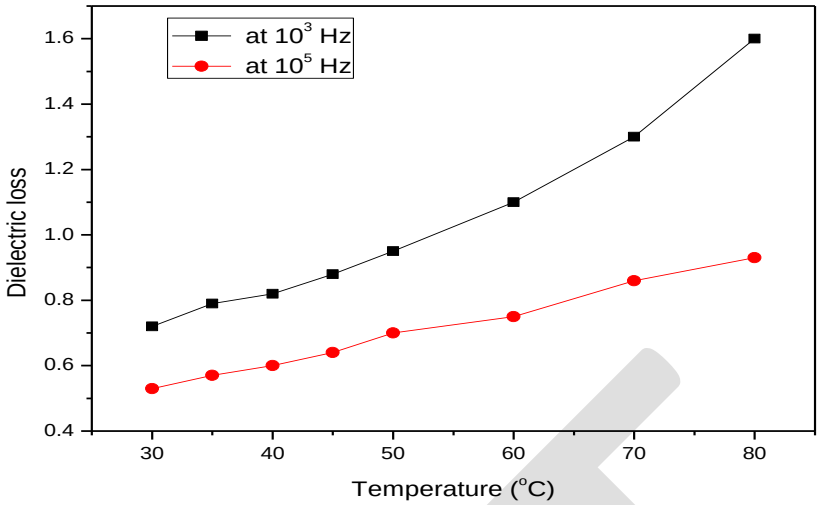

Fig.7: Variation of dielectric loss with temperature at frequencies of $10^3$and 10^5 Hz

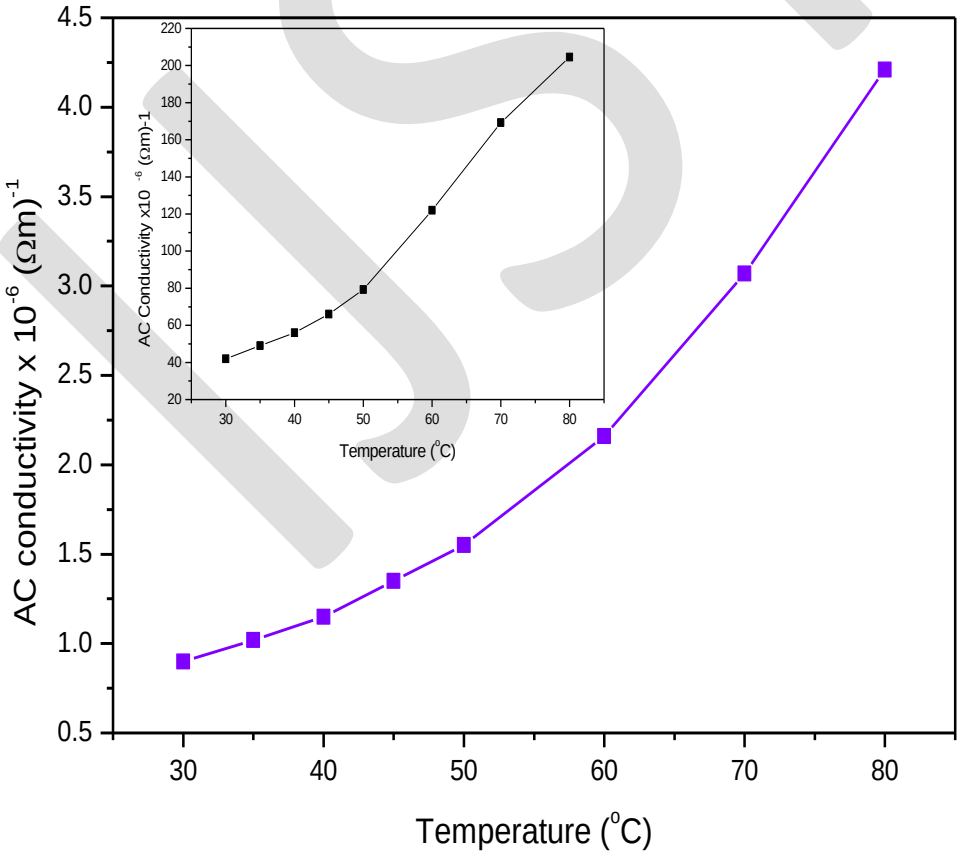

Fig.8: Variation of AC conductivity with temperature at 10^3 Hz for diglycine magnesium sulfate crystal, Inset: that at the frequency of 10^5 Hz

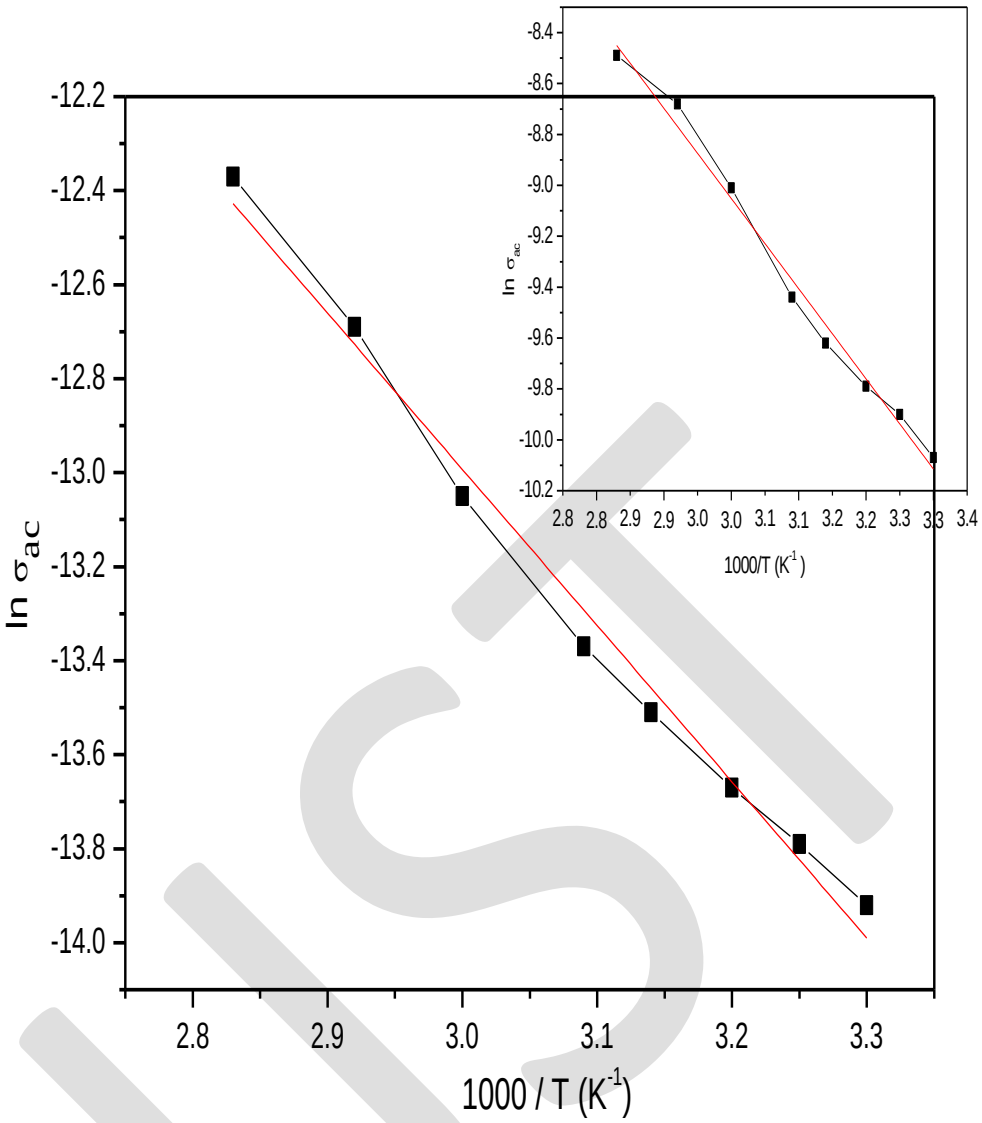

Fig.9: Plot of ln σ_{ac} versus 1/T at 10^3 Hz for diglycine magnesium sulfate crystal, Inset: the same at the frequency of 10^5 Hz

3.6 Measurement of third-order NLO parameters by Z-scan technique

Z-scan measurement is used to measure the nonlinear refractive index, third-order susceptibility and the nonlinear absorption coefficient via the closed and open aperture methods. In the closed aperture method, an aperture is placed to prevent some of the light from reaching the detector. A lens focuses a laser to a certain point, and after this point the beam naturally defocuses. After a further distance an aperture is placed with a detector behind it. The aperture causes only the central region of the cone of light to reach the detector. The detector is sensitive to any focusing or defocusing that a sample may induce. The sample is typically placed at the focus point of the lens, and then moved along the Z-axis. Open aperture method is similar to the above method, however the aperture is removed or enlarged to allow all the light to reach the detector. Open aperture method is used to measure the nonlinear absorption coefficient[28,29].

The open aperture and closed aperture Z-scan curves for the sample are given in the figure 10. The closed aperture Z-scan curve is characterized by a prefocal transmittance maximum (peak) followed by a postfocal transmittance minimum (valley) intensity. The transmission difference between peak and valley (ΔT_{p-v}) is written in terms of phase shift. Linear transmittance aperture (S) is calculated using the relation

$$\mathbf{S = 1 - exp\left(\frac{-2r_a^2}{\omega_a^2}\right)}$$

where r_a is the radius of the aperture and ω_a is the beam radius at the aperture. The third-order nonlinear refractive index (n_2) of the crystal was calculated by following the relation.

$$n_2 = \Delta\phi / (K\, I_o\, L_{eff})$$

where I_o is the intensity of the laser beam at the focus (Z = 0) and $K = 2\pi / \lambda$ (λ is the wavelength of laser beam). Here the effective thickness (L_{eff}) can be calculated using the relation

$$L_{eff} = [1-\exp(-\alpha L)] / \alpha$$

where α is the linear absorption coefficient and L is the thickness of the sample.

Using the open aperture curves, the nonlinear absorption coefficient (β) can be calculated. The nonlinear absorption coefficient (β) can be calculated using the following relation

$$\boldsymbol{\beta = \frac{2\sqrt{2}\Delta T}{I_0 L_{eff}}}$$

where ΔT is the one peak value at the open aperture Z-scan curve. The value of β will be negative for saturable absorption and positive for two photon absorption process. The real and imaginary parts of the third order nonlinear optical suceptibility ($\chi^{(3)}$) are defined as

Real part of $\chi^{(3)} = (10^{-4}\varepsilon_o\, c^2\, n_o^2\, n_2) / \pi$ esu

Imaginary part of $\chi^{(3)} = (10^{-2}\varepsilon_o\, c^2\, n_o^2 \lambda\, \beta) / 4\pi^2$ esu

Absolute value of $\chi^{(3)}$ = [{Real part of $\chi^{(3)}$}^{2}+ {Imaginary part of $\chi^{(3)}$}^{2}]$^{1/2}$ (esu). Here ε_o is the vacuum permitivity, n_o is the linear refractive index of the sample and c is the velocity of the light in vacuum. Using the above equations, nonlinear refractive index, third-order susceptibility and the nonlinear absorption coefficient of the crystals could be determined [30]. He-Ne laser (λ = 632.8 nm) was used as the light source and focused by a lens of 22.5 cm focal length. The obtained values of third-order NLO parameters are given in the table 2. It is reported that the negative nonlinear refractive index of the sample shows transmittance peak followed by transmittance valley, but the positive nonlinear refractive index shows the transmittance valley followed by transmittance peak. It is observed from figure 10 (b) that the DGMS crystal has negative nonlinear refractive index because the sample show transmittance peak followed by transmittance valley and therefore the sample shows the self-defocusing behaviour. Due to π-electron cloud movement from the donor to the acceptor of the grown crystal, the saturation absorption nature is revealed. The results of nonlinear absorption and nonlinear refraction of the sample reveals that these phenomena always coexist as they result from the same physical mechanisms. The physical processes that give rise to nonlinear absorption and the accompanying nonlinear refraction include ultrafast bound electronic processes where the response times are dictated by the characteristic formation and decay times of the optically induced excited states, thermal refraction, etc. This study helps to find the materials for optical switching and sensor protection applications in connection with both nonlinear absorption and nonlinear refraction and to understand the third-order NLO phenomena [31].

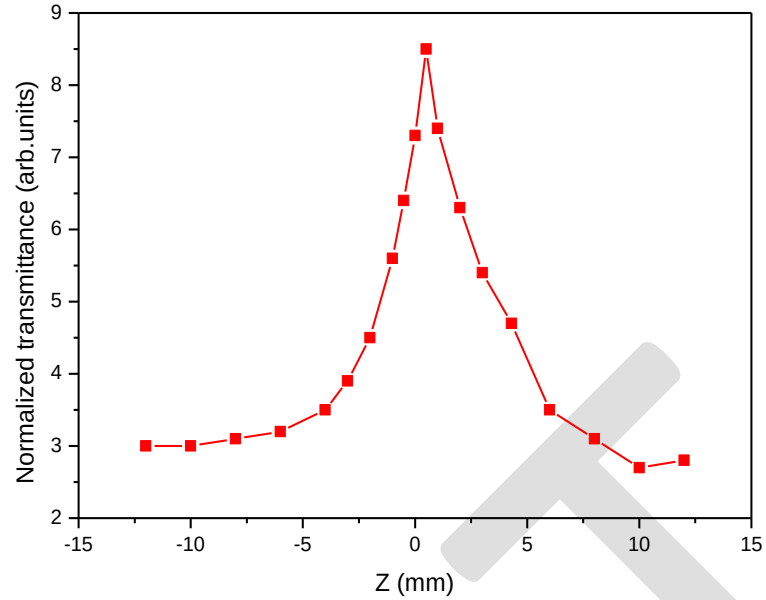

(a)

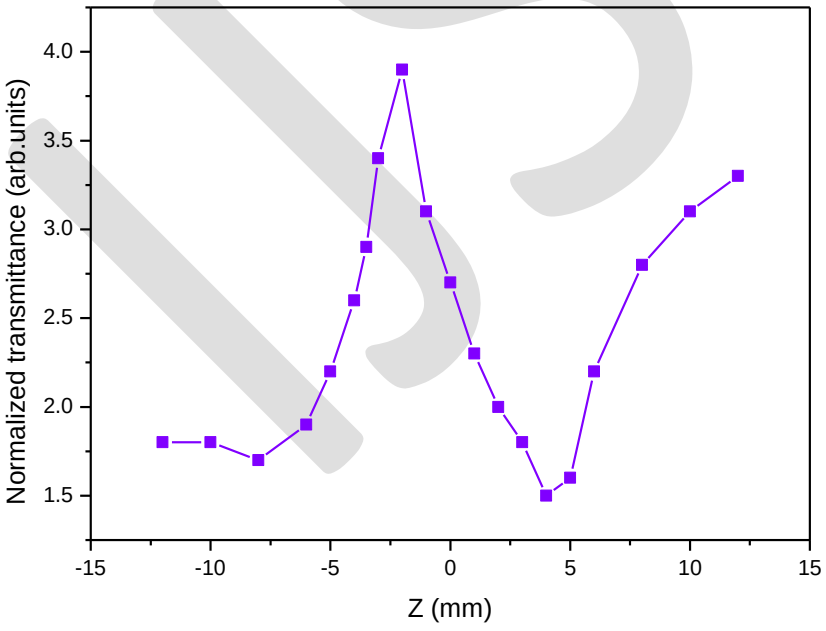

(b)

Fig.10: Z-scan curves: (a) in open aperture mode and (b) in closed aperture mode

Table 2: Third-order NLO parameters of DGMS cystal

Nonlinear refractive index (n_2)	1.75×10^{-10} c m^2/ W
Nonlinear absorption coefficient (β)	2.83×10^{-5} c m/W
The third-order nonlinear susceptibility ($\chi^{(3)}$	4.37×10^{-6} esu

3.7 UV-visible spectral studies

UV-visible transmittance spectrum of DGMS crystal is shown in the figure 11. From the results, it is confirmed that the sample is transparent in the visible-NIR regions. Absorbance or optical density is a measure of the capacity of the sample to absorb light of a specified wavelength and it is equal to the logarithm of the reciprocal of the transmittance and reflectance is a measure of the ability of a surface of the sample to reflect light. The absorbance and reflectance spectra of the sample are given in the figure 12. It is observed from the results that transmittance, reflectance and absorbance are equal to 100% at any wavelength and it is mentioned here that the scattering in percentage is negligibly small from a transparent crystal. Using the values of transmittance, the linear absorption coefficient (α) was determined using the relation $\alpha = (1/t) \ln (1/T)$ where T and t are the transmittance and thickness of the sample. The Tauc's relation connecting the absorption coefficient (α) and photon energy (hν) is $(\alpha h\nu)^2 = A (h\nu - E_g)$ where E_g is optical band gap of the crystal and A is a constant [32,33]. The Tauc's plot is drawn between $(\alpha h\nu)^2$ and hν and it is presented in the figure 13. From the figure, it is noticed that the optical band gap of the grown DGMS crystal is 4.98 eV.

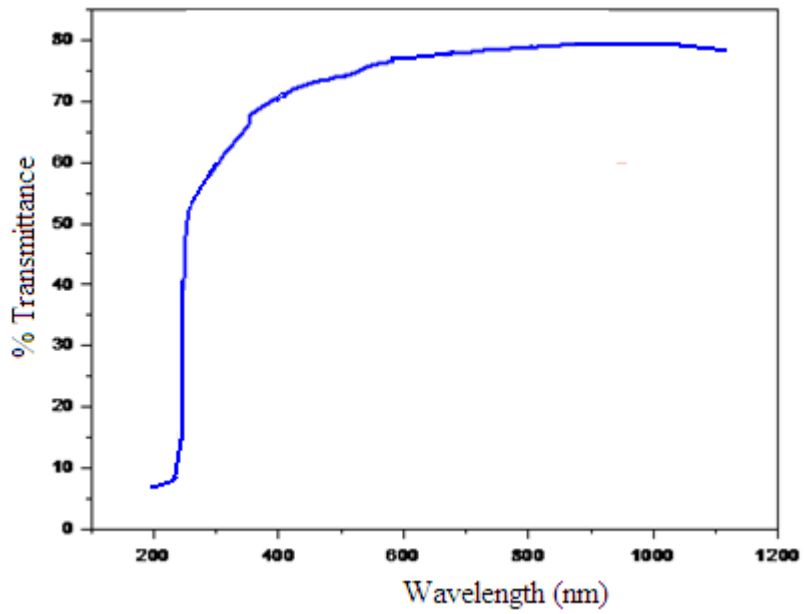

Fig.11: Optical transmittance spectrum of DGMS crystal

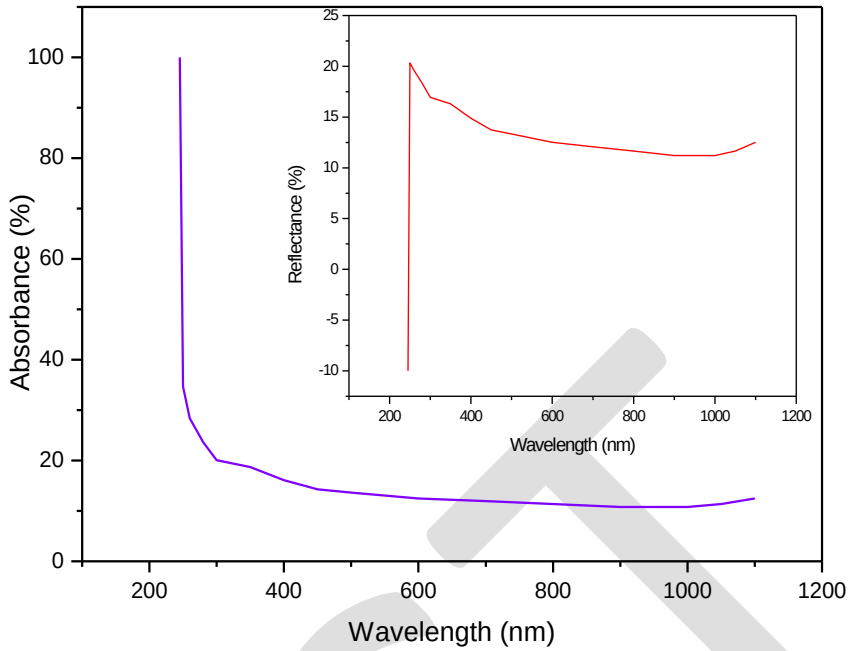

Fig.12: Absorbance and reflectance spectra for DGMS crystal

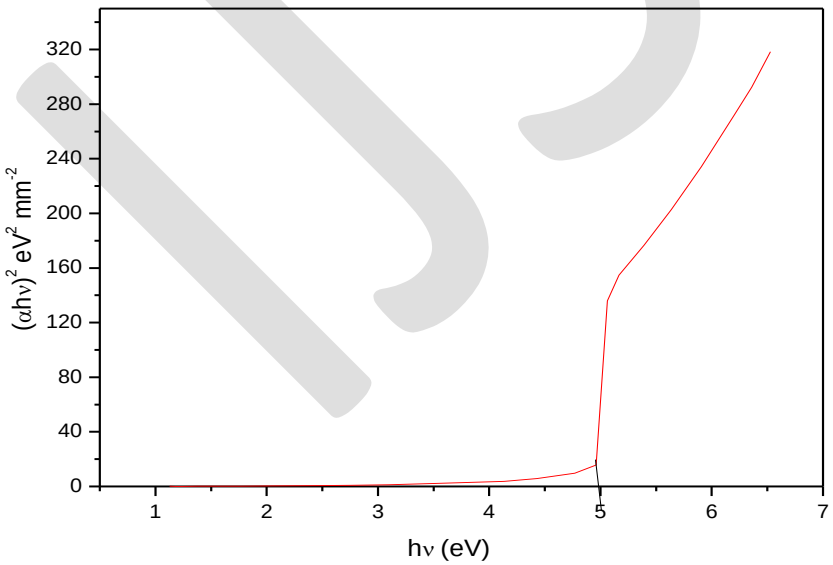

Fig.13: Tauc's plot for DGMS crystal

3.8 EDAX and CHN analysis

Energy Dispersive Analysis by X-rays (EDAX) technique a chemical microanalysis method used in conjunction with scanning electron microscopy (SEM). This technique detects X-rays emitted from the sample during bombardment by an electron beam to characterize the elemental composition of the sample. The data generated by EDAX analysis

consist of spectra showing peaks corresponding to the elements making up the true composition of the sample being analyzed. The EDAX spectrum for the sample is presented in the figure 14. From the results it is confirmed that the elements such as carbon, oxygen, magnesium, sulphur and nitrogen are present in the DGMS sample. The weight percentage of hydrogen in the sample was obtained by CHN analysis. The weight percentage of the different elements in the sample is given in the table 3.

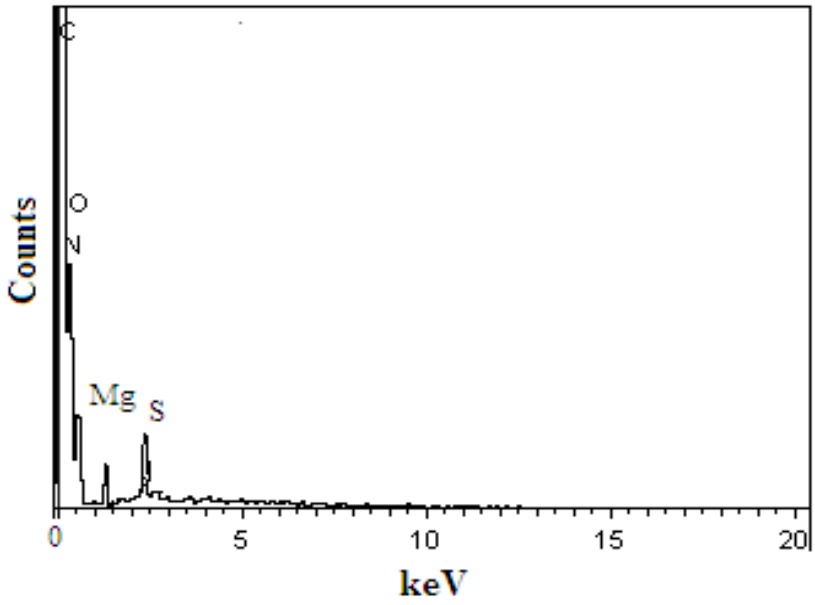

Fig.14: EDAX spectrum of DGMS crystal

Table 3: Weight percentage of elements in DGMS crystal

Element	Weight (%)
C	16.65
N	4.19
O	9.71
H	49.91
Mg	8.42
S	11.11

3.9 Measurement of laser damage threshold (LDT) value

The laser damage in the crystals are caused by various physical processes such as electron avalanche, multiphoton absorption and photoionization for the transparent materials whereas in case of high absorbing materials, the damage threshold is mainly due to the temperature rise, which leads to strain-induced fracture. It also depends upon the specific properties of material, pulse width, and wavelength of laser used. Laser damage threshold (LDT) studies for the sample were carried out using an Nd:YAG laser (1064 nm, 18 ns pulse width). The energy of the laser beam was measured by Coherent energy/power meter (Model No. EPM 200). LDT value is determined using the formula $P= E/ \tau\pi r^2$ where τ is the pulse width in ns, E is the input energy in mJ, r is radius of the spot in mm [34]. The obtained value of LDT of the sample is 0.387 GW/cm^2 . The value of LDT for grown crystal is more than that of KDP crystal (0.20 GW/cm^2) crystal.

4. Conclusions

Single crystals of diglycine magnesium sulfate (DGMS) were grown successfully by slow solvent evaporation technique. Solubility and nucleation curves for the sample were obtained as a function of temperature. XRD method was used to find the crystal structure of the grown DGMS crystal as triclinic structure. Mechanical strength of the sample was analyzed by measuring hardness, yield strength and stiffness constant.LDT value of DGMS crystal was measured to be 0.387 GW/cm^2. The low values of dielectric constant and loss factor of DGMS crystal are the desirable parameters for third-order NLO devices. AC conductivity and activation energy were evaluated using the data obtained from the dielectric studies. Third-order NLO parameters such as nonlinear refractive index, third-order susceptibility and the nonlinear absorption coefficient were evaluated for DGMS crystal using open aperture and closed aperture Z-scan curves. The optical band gap of DGMS crystal was found to be 4.98 eV from Tauc's plot. Weight percentages of various elements present in the sample were found out by EDAX and CHN methods.

Acknowledgments

The authors like to thank the staff members of Cochin University (Cochin), Crescent Engineering College (Chennai), St.Joseph's College (Trichy), IIT (Madras), VIT(Vellore) and M.K.University (Madurai) for having helped us to carry out the research work.

References

[1] Xiue Ren, Dongli Xu, Dongfeng Xue, J. Crystal Growth 310 (2008) 2005.
[2] Dongli Xu, Dongfeng Xue, J. Crystal Growth 310 (2008) 2157.
[3] L. Misoguti, V.S. Bagnato, S.C. Zilio, A.T. Varela, F.D. Nunes, F.E.A. Melo, J. Mendes Filho, Opt. Mater. 6 (1996) 147.
[4] D. Eimert, S. Velsko, L. Davis, F.Wang, G. Loiaceono, G. Kennedy, IEEE J. Quantum Electron. 25 (1989) 179.
[5] M.D. Aggarwal, J. Choi,W.S.Wang, K. Bhat, R.B. Lal, A.D. Shield, B.G. Penn, D.O. Frazier, J. Crystal Growth 204 (1999) 179.
[6] P.Selvarajan, J.Glorium ArulRaj, S.Perumal J. Crystal Growth 311 (2009) 3835.
[7] D. Rajan Babu, D. Jayaraman, R. Mohan Kumar, R. Jayavel, J. Crystal Growth (2002) 121.
[8] G. Ramesh Kumar, S. Gokul Raj, R. Sankar, R. Mohan, S. Pandi, R. Jayavel, J. Crystal Growth 7 (2004) 213.
[9]M. Lenin a, G. Bhavannarayana b, P. Ramasamy Optics Communications 282 (2009) 1202.
[10] A.S.J. Lucia Rose, P. Selvarajan, S. Perumal Spectrochimica Acta Part A 81 (2011) 270.
[11] S.Hoshino, T.Mitsui, F.Jona, R.Pepinsky, Phys.Rev.115 (1959) 323.
[12] Hung-Wen Li, Gu-Shen Yu, Herbert L. Strauss, J. Phys. Chem. B 102 (1998) 298.
[13] S. Natarajan, K. Ravikumar, S.S. Rajan, Z. Kristallogr. 168 (1984) 75.
[14] Tapati Mallik, Tanusree Kar, Cryst. Res. Technol. 40 (2005) 778.
[15] R. Muralidharan, R. Mohankumar, P.M. Ushasree, R. Jayavel, P. Ramasamy, J. Crystal Growth 234 (2002) 545.
[16] T. Balakrishnan, K. Ramamurthi, Cryst. Res. Technol. 41 (2006) 1184.
[17] R. Ezhil Vizhi, S. Kalainathan, G. Bhagavannarayana, Cryst. Res. Technol. 42 (2007) 1104.
[18] D. Sajan, N. Vijayan, K. Safakath Reji Philip, Hubert Joe, J. Phys. Chem. A 115 (2011) 8216.

[19] T. Uma Devi, N. Lawrence, R. Ramesh Babu, K.R. Ramamurthy, G. Bagavannarayana, J. Miner. Mater. Charact. Eng. 8 (2009) 755.
[20] P.V. Dhanaraj, Santheep K. Mathew, N.P. Rejesh, J. Crystal Growth 310 (2008) 2532.
[21] Jaroslav Nyvlt, Rudolf Rychly, Jaroslav Gottfried, Jirina Wurzelova, J. Crystal Growth, 6 (2) (1970) 151.
[22] S.K. Kurtz, T.T. Perry, J. Appl. Phys. 39 (1968) 3798.
[23]S. Suresh, A. Ramanand, D. Jayaraman, Optoelectronics and advanced materials,Rapid Commun. 4 (12) (2010) 1987.
[24]W.A. Wooster, Physical properties and atomic arrangements in crystals, Rep.Prog. Phys. 16 (1953) 62.
[25].K.V. Rao, A. Samakula, Journal. Appl. Phys. 36 (1965) 2031.
[26] A.S.J.Lucia Rose, P.Selvarajan,S.Perumal, Physica B 406 (2011) 412.
[27] P.Selvarajan, B.N. Das, H.B. Gon, K.V. Rao, Journal. Mater. Sci. 29 (1994) 4061.
[28]T. Xia, D.J. Hagan, M. Sheik-Bahae, and E.W. Van Stryland, Opt. Lett. 19 (1994) 317.
[29] T.Kanagasekaran, Mythili, P. Srinivasan, P. Nooraldeen, A. Y. Palanisamy, P. K. Gopalakrishnan, R., Cryst. Growth Des. 8 (2008) 2335.
[30] P.B. Chapple, J. Staromlynska and R.G. McDuff, J. Opt. Soc. Am B. 11 (1994) 975.
[31]R. Jothi Mani, P.Selvarajan, H. Alex Devadoss, D. Shanthi, Optik 126 (2015) 213.
[32] S.H. Wemple, D. DiDomenico, Phys. Rev. B 3 (4) (1971) 1338.
[33] J.C. Tauc et al., Optical Properties of Solids, Amsterdam, North-Holland (1972).
[34]Redrothu Hanumantharao, S.Kalainathan, Optik, 124 (2013) 2204.